Layer-by-Layer Electrostatic Self-Assembly of Single-Wall Carbon Nanotube Polyelectrolytes

ARTICLE *in* LANGMUIR · FEBRUARY 2006

Impact Factor: 4.46 · DOI: 10.1021/la051736i · Source: PubMed

Layer-by-Layer Electrostatic Self-Assembly of Single-Wall Carbon Nanotube Polyelectrolytes

Hanna Paloniemi,*,†,§ Marjo Lukkarinen,† Timo Ääritalo,† Sami Areva,‡ Jarkko Leiro,|| Markku Heinonen,|| Keijo Haapakka,† and Jukka Lukkari*,†

Department of Chemistry, University of Turku, 20014 Turku, Finland, Graduate School of Materials Research, Turku, Finland, Department of Physical Chemistry, Åbo Akademi University, 20500 Turku, Finland, and Laboratory of Materials Science, University of Turku, 20014 Turku, Finland

Received June 28, 2005. In Final Form: September 23, 2005

We have used anionic and cationic single-wall carbon nanotube polyelectrolytes (SWNT-PEs), prepared by the noncovalent adsorption of ionic naphthalene or pyrene derivatives on nanotube sidewalls, for the layer-by-layer self-assembly to prepare multilayers from carbon nanotubes with polycations, such as poly(diallyldimethylammonium) or poly(allylamine hydrochloride) (PDADMA or PAH, respectively), and polyanions (poly(styrenesulfonate), PSS). This is a general and powerful technique for the fabrication of thin carbon nanotube films of arbitrary composition and architecture and allows also an easy preparation of all-SWNT (SWNT/SWNT) multilayers. The multilayers were characterized with vis−near-IR spectroscopy, X-ray photoelectron spectroscopy (XPS), surface plasmon resonance (SPR) measurements, atomic force microscopy (AFM), and imaging ellipsometry. The charge compensation in multilayers is mainly intrinsic, which shows the electrostatic nature of the self-assembly process. The multilayer growth is linear after the initial layers, and in SWNT/polyelectrolyte films it can be greatly accelerated by increasing the ionic strength in the SWNT solution. However, SWNT/SWNT multilayers are much more inert to the effect of added electrolyte. In SWNT/SWNT multilayers, the adsorption results in the deposition of 1−3 theoretical nanotube monolayers per adsorbed layer, whereas the nominal SWNT layer thickness is 2−3 times higher in SWNT/polyelectrolyte films prepared with added electrolyte. AFM images show that the multilayers contain a random network of nanotube bundles lying on the surface. Flexible polyelectrolytes (e.g., PDADMA, PSS) probably surround the nanotubes and bind them together. On macroscopic scale, the surface roughness of the multilayers depends on the components and increases with the film thickness.

Introduction

Carbon nanotubes are one-dimensional tubular forms of carbon, which can be either multiwalled or single-walled (MWNTs or SWNTs, respectively). They possess unique electronic, mechanical, and thermal properties, which suggest a wide range of applications in materials science, sensor technology, and biomedical applications.[1] However, the possible applications set other criteria for useful materials, too. In many cases the material is needed in the form of a thin uniform film on a substrate of choice, requiring facile methods for the controlled thin film fabrication. On the other hand, for composite materials the good miscibility of the components is of vital importance. Especially, SWNTs can act as reinforcement in polymer composites due to their exceptional mechanical strength and thermal stability, but the phase segregation of the components leads to deteriorated properties.[2] Both requirements emphasize the importance of materials processing and manipulation at the molecular level. Carbon nanotubes can be prepared in a number of ways but the fundamental limitation to the use of the pristine material is its intractability as the very high attraction between individual nanotubes leads to the formation of large bundles and ropes and, therefore, insolubility in common solvents. In addition, single-wall carbon nanotubes have a flexible structure and a highly anisotropic shape making their molecular level manipulation and ordering harder than that of spherical and rigid objects. These factors hamper their manipulation at the molecular level and the development of controlled solution-phase deposition and self-assembly methods.

The insolubility of pristine nanotubes creates a need for their chemical modification. Solubility in organic or aqueous media can be obtained by covalent functionalization of the side walls or oxidative cutting of the tubes.[3] This approach, however, sacrifices the electronic properties of the nanotubes or their extremely high aspect ratio, which is important for, e.g., mechanical properties. Another approach is to suspend nanotubes in solutions with surfactants or by physically adsorbing solubilizing components on the side walls.[4] These noncovalent modification techniques retain the desired properties of the nanotubes, simultaneously rendering the material processible even in aqueous medium.

The establishment of reliable fabrication methods for homogeneous thin films of SWNTs and polymers is important for the

* Corresponding authors. Telephone: +358-(0)2-3336713 (H.P.); +358-(0)2-3336712 (J.L.). E-mail: hanna.paloniemi@utu.fi (H.P.); jukka.lukkari@utu.fi (J.L.).

† Department of Chemistry, University of Turku.

§ Graduate School of Materials Research.

‡ Åbo Akademi University.

|| Department of Physics, University of Turku.

(1) (a) Terrones, M. *Annu. Rev. Mater. Res.* **2003**, *33*, 419. (b) Ouyang, M.; Huang, J.-L.; Lieber, C. M. *Acc. Chem. Res.* **2002**, *35*, 1018. (c) Avouris, P. *Acc. Chem. Res.* **2002**, *35*, 1026. (d) Sun, Y.-P.; Fu, K.; Lin, Y.; Huang, W. *Acc. Chem. Res.* **2002**, *35*, 1096. (e) Kam, N. W. S.; Dai, H. *J. Am. Chem. Soc.* **2005**, *127*, 6021.

(2) See, e.g.: (a) Dyke, C. A.; Tour, J. M. *J. Phys. Chem. A* **2004**, *108*, 11151. (b) Blake, R.; Gun'ko, Y. K.; Coleman, J.; Cadek, M.; Fonseca, A.; Nagy, J.; Blau, W. J. *J. Am. Chem. Soc.* **2004**, *126*, 10226. (c) Cadek, M.; Coleman, J. N.; Ryan, K. P.; Nicolosi, V.; Bister, G.; Fonseca, A.; Nagy, J. B.; Szostak, K.; Béguin, F.; Blau, W. J. *Nano Lett.* **2004**, *4*, 353. (d) Dalton, A. B.; Collins, S.; Muñoz, E.; Razal, J. M.; Ebron, V. H.; Ferraris, J. P.; Coleman, J. N.; Kim, B. G.; Baughman, R. H. *Nature* **2003**, *423*, 703. (e) Mamedov, A. A.; Kotov, N. A.; Prato, M.; Guldi, D. M.; Wicksted, J. P.; Hirsch, A. *Nat. Mater.* **2002**, *1*, 190. (f) Lillehei, P. T.; Park, C.; Rouse, J. H.; Siochi, E. J. *Nano Lett.* **2002**, *2*, 827.

(3) (a) Hirsch, A.; Vostrowsky, O. *Top. Curr. Chem.* **2005**, *245*, 193. (b) Tour, J. M.; Dyke, C. A. *Chem. Eur. J.* **2004**, *10*, 812. (c) Tasis, D.; Tagmatarchis, N.; Georgakilas, V.; Prato, M. *Chem. Eur. J.* **2003**, *9*, 4000. (d) Hirsch, A. *Angew. Chem., Int. Ed.* **2002**, *41*, 1853.

10.1021/la051736i CCC: $33.50
Published on Web 11/19/2005

development of nanoscale devices and sensors. Furthermore, methods to assemble SWNTs into layered structures without foreign materials or polymer additives are needed. Thin films of pure carbon nanotubes have been prepared, e.g., by solution casting, electrophoretic deposition, electrodeposition using electroactive surfactants, precipitation from a superacid solution, nucleation from a locally supersaturated suspension, dip coating, adsorption on modified surfaces, filtering on a dissolvable membrane, and Langmuir−Blodgett technique.[5] However, the techniques employed often suffer from nonuniform film coverage or a lack of control of the film properties or do not easily allow for the generation of complex film architectures with several different components.

Perhaps the most versatile thin film fabrication technique today is the layer-by-layer electrostatic self-assembly (LbL), which produces robust films and allows precise control over the film thickness and its properties.[6] This technique allows the stepwise fabrication of multilayers containing various functionalities in a predesigned, vertical order. In the LbL deposition method positively and negatively charged species are adsorbed successively, and the method is based on the surface charge reversal after the adsorption of each layer. This technique was first demonstrated with polyelectrolytes, but it has since been employed for nucleic acids,[7a] proteins,[7b] ionic dyes,[7c] nanoparticles,[7d] and even viruses.[7e] Film thickness can be controlled in a precise manner, since each layer usually contributes a known increase in thickness.

While hydrophobic[8a] and charge-transfer interactions[8b] and hydrogen bonding[8c] have been used in the LbL technique, the electrostatic self-assembly is the most versatile and facile method. Multiwalled carbon nanotubes (MWNTs) covalently modified with PSS and poly(acrylic acid) have been used as templates for polyelectrolyte multilayer self-assembly.[9] Nonmodified carbon nanotubes are electrically neutral, but oxidatively shortened MWNTs possess anionic groups (mainly carboxylates) at the open tube ends but also at defect sites generated along the tube surface. The cut and/or carboxylated MWNTs can interact electrostatically with polycations, e.g., with poly(diallyldimethylammonium) (PDADMA), and can be incorporated in PDADMA/MWNT multilayers.[10] Extensive oxidation necessary for the generation of a large ionic surface charge density, however, destroys the electronic properties of the nanotubes and sacrifices one of their principal properties, the high aspect ratio. Similarly treated SWNTs also carry negative charges due to carboxylic acid moieties at the ends and side walls and allow multilayer buildup or nanoparticle formation with positively charged polymers, e.g. PDADMA and poly(ethyleneimine) (PEI).[2,11−13] Despite the loss of the characteristic electronic structure with the van Hove transitions, the charge density of oxidized SWNTs is still rather low and may necessitate the incorporation of "glue layers" at regular intervals in the film structure.[2] In fact, the shorter and more defect-rich nanotubes are preferentially incorporated into the multilayer during the layer-by-layer assembly process. In addition, a recent work suggests that the interaction of PDADMA with nanotubes is not electrostatic in nature but due to $\pi-\pi$ interactions between PDADMA impurities and the tube side walls.[14] Two procedures have been recently reported for the self-assembly of polyelectrolytes onto or with nonoxidized, full-length SWNTs.[15,16] Rouse et al. use SWNTs suspended in dimethylformamide (DMF) and their charge-transfer interactions with amines to build multilayers with PEI, poly(allylamine), and poly(4-vinylpyridine) (PAH and P4VP, respectively). These films exhibited linear growth and preserved the electronic structure of the nanotubes. On the other hand, noncovalent modification of SWNTs with 1-pyrenepropylamine enabled the successive layer-by-layer deposition of polyanions and polycations on nanotubes grown and suspended on transmission electron microscopy (TEM) grids. Recently, positively charged SWNTs have been prepared by treatment with methylene blue or grafting with poly(4-vinylpyridine) and assembled with poly(styrenesulfonate), PSS, or poly(acrylic acid), PAA, respectively.[17]

Despite several works dealing with the preparation of ultrathin films with carbon nanotubes, a general, versatile, and facile method for the fabrication of SWNT films with practically arbitrary architecture and composition has not been reported. This could be realized using the sequential electrostatic layer-by-layer deposition technique, but it would require the use of nanotubes with a truly polyelectrolyte-type nature. We have recently reported the fabrication and characterization of full-length single-wall carbon nanotube polyelectrolytes (SWNT-PEs) based on the noncovalent modification of SWNTs with

(4) (a) Islam, M. F.; Rojas, E.; Bergey, D. M.; Johnson, A. T.; Yodh, A. G. *Nano Lett.* **2003**, *3*, 269. (b) Li, H.; Zhou, B.; Lin, Y.; Gu, L.; Kang, W.; Shiral Fernando, K. A.; Kumar, S.; Allard, L. F.; Sun, Y.-P. *J. Am. Chem. Soc.* **2004**, *126*, 1014. (c) Chen, R. J.; Zhang, Y.; Wang, D.; Dai, H. *J. Am. Chem. Soc.* **2001**, *123*, 3838. (d) Nakashima, N.; Tomonari, Y.; Murakami, H. *Chem. Lett*. **2002**, *31*, 638. (e) Xin, H.; Woolley, A. T. *J. Am. Chem. Soc.* **2003**, *125*, 8710. (f) Gómez, F. J.; Chen, R. J.; Wang, D.; Waymouth, R. M.; Dai, H. *J. Chem. Soc., Chem. Commun*. **2003**, 190. (g) Petrov, P.; Stassin, F.; Pagnoulle, C.; Jérôme, R. *J. Chem. Soc., Chem. Commun*. **2003**, 2904. (h) Liu, L.; Wang, T.; Li, J.; Guo, Z.-X.; Dai, L.; Zhang, D.; Zhu, D. *Chem. Phys. Lett*. **2003**, *367*, 747. (i) Shiral Fernando, K. A.; Lin, Y.; Wang, W.; Kumar, S.; Zhou, B.; Xie, S.-Y.; Cureton, L. T.; Sun, Y.-P. *J. Am. Chem. Soc*. **2004**, *126*, 10234. (j) Guldi, D. M.; Rahman, G. M. A.; Jux, N.; Balbinot, D.; Hartnagel, U.; Tagmatarchis, N.; Prato, M. *J. Am. Chem. Soc*. **2005**, *127*, 9830. (k) Zhang, J.; Lee, J.-K.; Wu, Y.; Murray, R. W. *Nano Lett.* **2003**, *3*, 403.

(5) (a) Meitl, M. A.; Zhou, Y.; Gaur, A.; Jeon, S.; Usrey, M. L.; Strano, M. S.; Rogers, J. A. *Nano Lett.* **2004**, *4*, 1643. (b) Gao, B.; Yue, G. Z.; Qiu, Q.; Cheng, Y.; Shimoda, H.; Fleming, L.; Zhou, O. *Adv. Mater*. **2001**, *13*, 1770. (c) Nakashima, N.; Kobae, H.; Sagara, T.; Murakami, H. *ChemPhysChem* **2002**, *5*, 456. (d) Sreekumar, T. V.; Liu, T.; Kumar, S.; Ericson, L. M.; Hauge, R. H.; Smalley, R. E. *Chem. Mater*. **2003**, *15*, 175. (e) Shimoda, H.; Oh, S. J.; Geng, H. Z.; Walker, R. J.; Zhang, X. B.; McNeil, L. E.; Zhou, O. *Adv. Mater*. **2002**, *14*, 899. (f) Spotnitz, M. E.; Ryan, D.; Stone, H. A. *J. Mater. Chem.* **2004**, *14*, 1299. (g) Zhu, J.; Yudasaka, M.; Zhang, M.; Kasuya, D.; Iijima, S. *Nano Lett.* **2003**, *3*, 1239. (h) Wu, Z.; Chen, Z.; Du, X.; Logan, J. M.; Sippel, J.; Nikolou, M.; Kamaras, K.; Reynolds, J. R.; Tanner, D. B.; Hebard, A. F.; Rinzler, A. G. *Science* **2004**, *305*, 1273. (i) Di Luccio, T.; Antolini, F.; Aversa, P.; Scalia, G.; Tapfer, L. *Carbon* **2004**, *42*, 1119. (j) Guo, Y.; Wu, J.; Zhang, Y. *Chem. Phys. Lett*. **2002**, *362*, 314. (k) Guo, Y.; Minami, N.; Kazaoui, S.; Peng, J.; Yoshida, M.; Miyashita, T. *Physica B* **2002**, *323*, 235.

(6) (a) Decher, G. *Science* **1997**, *277*, 1232. (b) Decher, G., Schlenoff, J. B., Eds. *Multilayer Thin Films. Sequential Assembly of Nanocomposite Materials*; Wiley-VCH: Weinheim, Germany, 2003.

(7) (a) Marx, K. A. *Biomacromolecules* **2003**, *4*, 1099. (b) Lvov, Y. M.; Lu, Z.; Schenkman, J. B.; Zu, X.; Rusling, J. F. *J. Am. Chem. Soc*. **1998**, *120*, 4073. (c) Ariga, K.; Lvov, Y.; Kunitake, T. *J. Am. Chem. Soc.* **1997**, *119*, 2224. (d) Kotov, N. A.; Dekany, I.; Fendler, J. H. *J. Phys. Chem*. **1995**, *99*, 13065. (e) Lvov, Y.; Haas, H.; Decher, G.; Möhwald, H.; Mikhailov, A.; Mtchedlishvily, B.; Morgunova, E.; Vainshtein, B. *Langmuir* **1994**, *10*, 4232.

(8) (a) Lojou, E.; Bianco, P. *Langmuir* **2004**, 20, 748. (b) Shimazaki, Y.; Mitsuishi, M.; Ito, S.; Yamamoto, M. *Langmuir* **1997**, *13*, 1385. (c) Wang, L. Y.; Wang, Z. Q.; Zhang, X.; Shen, J. C.; Chi, L. F.; Fuchs, H. *Makromol. Rapid Commun*. **1997**, *18*, 509.

(9) Kong, H.; Luo, P.; Gao, C.; Yan, D. *Polymer* **2005**, *46*, 2472.

(10) (a) Kim, B.; Park, H.; Sigmund, W. M. *Langmuir* **2003**, *19*, 2525. (b) Kim, B.; Sigmund, W. M. *Langmuir* **2003**, *19*, 4848. (c) Zhang, M.; Yan, Y.; Gong, K.; Mao, L.; Guo, Z.; Chen, Y. *Langmuir* **2004**, *20*, 8781. (d) Correa-Duarte, M. A.; Olek, M.; Ostrander, J.; Jurga, S.; Möhwald, H.; Kotov, N.; Kempa, K.; Giersig, M. *Nano Lett*. **2004**, *4*, 1889. (e) Kosiorek, A.; Kandulski, W.; Giersig, M.; Liz-Marzán, L. M. *Chem. Mater*. **2005**, *17*, 3268.

(11) Rouse, J. H.; Lillehei, P. T. *Nano Lett*. **2003**, *3*, 59.

(12) He, P.; Bayachou, M. *Langmuir* **2005**, *21*, 6086.

(13) Kovtyukhova, N. I.; Mallouk, T. E. *J. Phys. Chem. B* **2005**, *109*, 2540.

(14) Yang, D.-Q.; Rochette, J.-F.; Sacher, E. *J. Phys. Chem. B* **2005**, *109*, 4481.

(15) Rouse, J. H.; Lillehei, P. T.; Sanderson, J.; Siochi, E. J. *Chem. Mater*. **2004**, *16*, 3904.

(16) Artyukhin, A. B.; Bakajin, O.; Stroeve, P.; Noy, A. *Langmuir* **2004**, *20*, 1442.

(17) (a) Yan, Y.; Zhang, M.; Gong, K.; Su, L.; Guo, Z.; Mao, L. *Chem. Mater* **2005**, *17*, 3457. (b) Qin, S.; Qin, D.; Ford, W. T.; Herrera, J. E.; Resasco, D. E. *Macromolecules* **2004**, *37*, 9963.

Chart 1. Ionic Naphthalene and Pyrene Derivatives Used in the Noncovalent Modification of SWNTs

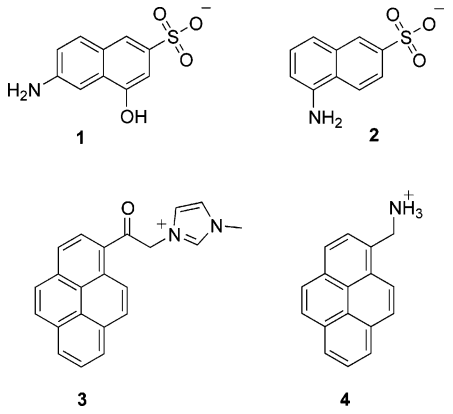

several polyaromatic ionic molecules.[18] These nanotubes retain their electronic properties and high aspect ratio and form aqueous solutions with high enough concentration and stability to be used in multilayer assembly. Depending on the ionic modifier, the neutral nanotube can be converted either to a highly charged polyanion or a polycation. Therefore, the polymeric components are not restricted to polycations, but anionic species can also be incorporated into the multilayers sequentially with SWNTs. This is important for polyionic species whose surface charge is pH-dependent, such as proteins. In addition, the use of cationic and anionic nanotubes makes possible the layer-by-layer fabrication of purely SWNT-based (all-SWNT) multilayers.

In this paper we demonstrate that the SWNT-PEs can be assembled from aqueous solutions on a variety of substrates by the LbL technique. We show that homogeneous SWNT/polyelectrolyte and SWNT/SWNT multilayers can be manufactured and characterize the multilayers using vis−near-IR spectroscopy, atomic force microscopy (AFM), and imaging ellipsometry. To our knowledge, this is the first time SWNTs have been electrostatically assembled to multilayers alone, without any polymer components.

Experimental Section

Materials. HiPco SWNTs (Carbon Nanotechnologies, Inc.) were purified by a thermal oxidation−acid extraction cycle and were turned into polyionic, water-soluble species via a noncovalent adsorption of the naphthalene and pyrene derivatives **1**−**4** (Chart 1) as described elsewhere.[18] Poly(diallyldimethylammonium chloride), M_w = 100 000−200 000 (PDADMA, Aldrich), was first dialyzed against 0.1 M NaBr to exchange the counteranions, and then the excess of NaBr was removed by dialysis against water. Poly(allylamine hydrochloride), M_w = 70 000 (PAH, Aldrich), poly(sodium *p*-styrenesulfonate), M_w = 70 000 (PSS, Aldrich), 3-aminopropyltriethoxysilane (APTES, Fluka, 96%), 2-mercaptoethanesulfonic acid, sodium salt (MESA, Aldrich, 98%), 2-mercaptoethylamine hydrochloride (MEA, Sigma), sodium bromide (NaBr, Riedel-de Haën, 99%), and sodium chloride (NaCl, Merck, 99%) were used as received. Microscopy glass slides (Menzel-Gläser) and silicon wafers (*p*-type, boron-doped, Okmetic, Finland) were used as substrate materials.

Multilayer Formation. To prepare SWNT/polyelectrolyte multilayers, anionic SWNT-PEs were alternately assembled with PDADMA or PAH and cationic SWNT-PEs with PSS (Chart 2). First, glass or silicon slides were cleaned in concentrated H_2SO_4/30% H_2O_2 (3:1) ("Piranha" solution. *Warning*! Piranha solution is very corrosive and must be treated with extreme caution; it reacts violently with organic material and must not be stored in tightly closed vessels.) and silanized with APTES in dry toluene solution (1% (v/v)) for 4 min at 60 °C to form a positively charged primer layer. Then, the slides were immersed alternately in a water solution of anionic SWNT-PEs (30 min immersion time) and PDADMA or PAH water solution (15 min). Doubling of the SWNT deposition time did not affect the results, and surface plasmon resonance measurements (vide infra) showed that the amount of nanotubes corresponding to a single layer will be adsorbed within 30−40 min (the difference in amount between 30 and 40 min was negligible, approximately 5% of the total). Therefore, the adsorption time of 30 min was considered sufficient for the formation of a SWNT monolayer. After each layer deposition, the substrate was rinsed with distilled water (3 × 1 min) and dried with N_2. For cationic SWNT-PEs, PSS was used as the counter polyelectrolyte. SWNT/SWNT multilayers were prepared by assembling alternately anionic and cationic SWNT-PEs with the procedure described above. The concentration of PDADMA, PAH, and PSS solutions was 10 mM with respect to the monomer, and the ionic strength was adjusted with NaBr (PDADMA and PSS) or NaCl (PAH) to 0.1 M. For anionic SWNT-PEs the ionic strength was adjusted to 0−0.2 M with NaBr, but no additional electrolyte was used with cationic SWNT-PEs. Multilayers were also prepared on evaporated gold surfaces. A 100 nm thick gold layer was evaporated on piranha-treated and silanized glass slides with an Edwards E306A coating system. A negatively charged MESA primer layer was formed by immersing the slides in a 1 mM MESA water solution for 1 h. SWNT/polyelectrolyte and SWNT/SWNT multilayers were built on the primed gold surface as described above. The kinetics of the adsorption of SWNT-PEs was studied by surface plasmon resonance (SPR) spectroscopy using an in situ flow cell (Spreeta, Texas Instruments). The gold electrode was cleaned with oxygen and hydrogen plasma before the cell assembly and then, before the measurements, with an aqueous solution of 1 wt % Triton X-100 and 0.11 M NaOH for 20 min. The cell was calibrated with distilled water (refractive index, 1.3330). The surface was modified with a MEA monolayer (1 mM solution, 1 h), rinsed with water, and filled with a 0.1 M NaBr solution.

Chart 2. Polymers Used in the Buildup of SWNT/Polyelectrolyte Multilayers

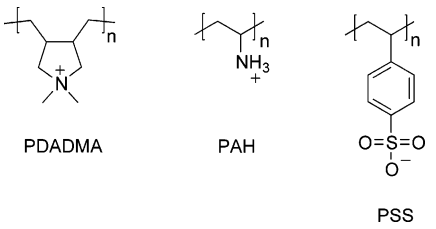

Multilayer Characterization. Vis−near-IR spectra were measured with a Varian Cary 5E spectrophotometer. X-ray photoelectron spectroscopy (XPS) spectra were recorded with a Perkin-Elmer PHI 5400 spectrometer using an electron takeoff angle of 60° and an analyzer pass energy of 89.45 eV for survey spectra or 35.75 eV for narrow-scan spectra. Monochromatic Al Kα radiation (E = 1486.6 eV) was used for photoexcitation. The surface morphology was determined by noncontact tapping mode atomic force microscopy (AFM) using a NanoScope III multimode AFM (Digital Instruments, Santa Barbara, CA) apparatus. The used ultrasharp silicon cantilever was 125 μm in length and had a resonance frequency of approximately 325 kHz. The tip height was 15−20 μm having a nominal radius of curvature less

(18) Paloniemi, H.; Ääritalo, T.; Laiho, T.; Liuke, H.; Kocharova, N.; Haapakka, K.; Terzi, F.; Seeber, R.; Lukkari, J. *J. Phys. Chem. B* **2005**, *109*, 8634.

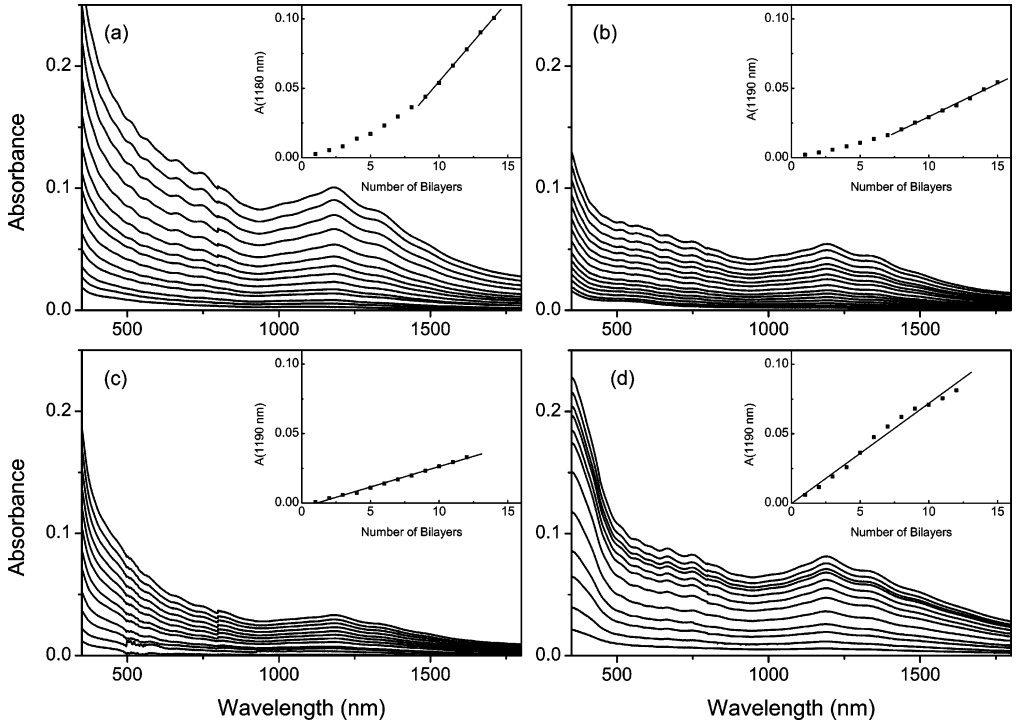

Figure 1. Growth of (a) SWNT**1**/PDADMA, (b) SWNT**2**/PDADMA, (c) SWNT**1**/PAH (pH 6.5 for PAH), and (d) PSS/SWNT**3** multilayers on glass. Spectra were measured after each SWNT layer deposition (ionic strength: 0.1 M with polylectrolytes, zero with SWNTs). The small discontinuity at 800 nm is due to the change of grating and detector. Insets: S_{11} peak intensity (1190 nm) vs the number of bilayers.

than 10 nm. All the AFM measurements were carried out in ambient air. Scanning electron microscopy images were obtained with a Cambridge Stereoscan 200 SEM equipped with a Link (AN) 10000 EDX system. Ellipsometric measurements were performed with a Nanofilm EP^3 imaging ellipsometer. In variable-angle measurements the angle of incidence was varied in the range of 45−55 (for samples on glass) or 50−60° (for samples on silicon or gold), and a laser source (532 nm) was used with a 10× objective. In spectral measurement the angle of incidence was fixed at 55 (glass) or 65° (silicon, gold), and a Xe lamp was used with a 2× objective in the spectral range of 370−810 nm. Surface maps were recorded with an angle of incidence of 55 (glass) or 60° (gold) and a Xe lamp source (532 nm) with a 2× objective.

Results and Discussion

SWNT/Polyelectrolyte Multilayers. Our initial approach was to study the incorporation of SWNT-PEs into multilayers of PDADMA, PAH, and PSS, since these polymers are being widely used in the layer-by-layer assembly of polyelectrolyte multilayers. The anionic and cationic SWNT-PEs with best stability and solubility were chosen for the multilayer fabrication based on our earlier work.[18] These nanotube polyelectrolytes have a linear ionic charge density similar to that of common highly charged polyelectrolytes, such as PDADMA and PSS. The deposition conditions for the polymers were adapted from literature, while those for the SWNT-PEs were optimized during this work. The progress of multilayer formation was followed by vis−near-IR spectroscopy after the deposition of each bilayer on glass. Examples of the growth of different SWNT/polyelectrolyte multilayers are shown in Figure 1. For SWNT**1**/PDADMA films the absorbance due to nanotubes increased slowly during the first 5−10 bilayers, after which the growth accelerated and became linear. Theoretically, multilayer growth should be linear if each adsorbed layer imparts a constant amount of charge to the growing film. However, during the very first layers the substrate affects the growth of the thin film, and in the literature on polyelectrolyte multilayers this part of the film is usually called zone I according to the widely accepted three-zone model.[19] The other zones constitute the bulk of the film (zone II) and the film/ambient interface (outer zone III). During the layer-by-layer buildup the zones I and III form first. After that their thickness remains constant and further film growth results in the gradual increase of the zone II. Therefore, these results indicate that with SWNT**1**/PDADMA multilayers the formation of zone II starts only after ca. 8−10 bilayers. Regular linear layer growth was also observed for SWNT**2**/PDADMA multilayers, and the width of zones I + III is comparable to that in the SWNT**1**/PDADMA multilayers. It is noteworthy that the van Hove transitions (S_{11}, S_{22}, and M_{11}) are clearly visible in the spectra of both multilayers, indicating that the electronic structure of the incorporated SWNTs remains intact in the films. We have previously shown that the ionic surface charge density of SWNT**2** is greater than that of SWNT**1**, suggesting that less nanotubes are required to neutralize the positive charge of PDADMA in multilayers. In fact, comparison of Figure 1a,b shows that the amount of nanotube material per bilayer is smaller with the nanotube polyelectrolyte SWNT**2**.

SWNT/polyelectrolyte multilayers can also be fabricated with PAH, a weak polyelectrolyte. PAH has an effective pK_a of ca. 8−9, being fully protonated in neutral and acidic solutions but partly deprotonated in slightly basic solutions.[20] Rouse et al. have recently shown that SWNT/PAH multilayers can be formed from DMF solution via donor−acceptor interactions.[15] However, multilayers can also be deposited in acidic or neutral aqueous solutions (pH of the PAH solution 3.1 or 6.5), in which the amino groups of PAH are fully protonated, indicating the prevalence of electrostatic interactions between the components (Figures 1c and S2 (Supporting Information)). The growth of

(19) Ladam, G.; Schaad, P.; Voegel, J. C.; Schaaf, P.; Decher, G.; Cuisinier, F. *Langmuir* **2000**, *16*, 1249.
(20) Choi, J.; Rubner, M. F. *Macromolecules* **2005**, *38*, 116.

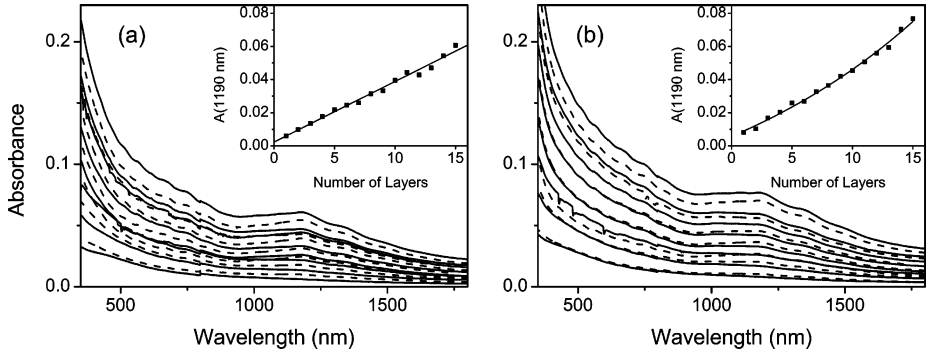

Figure 2. (a) SWNT**1**/SWNT**3**, and (b) SWNT**1**/SWNT**4** multilayer growth up to 15 layers. Salt (0.10 or 0.15 M NaBr) was added to the SWNT**1** solution in a or b, respectively (no added electrolyte in the SWNT**3** or SWNT**4** solutions). Insets: S_{11} peak intensity (1190 nm) vs the number of nanotube layers.

SWNT**1**/PAH multilayers is regular and linear, but the amount of adsorbed material is relatively small compared to the SWNT/PDADMA multilayers. This is in accordance with the small and practically pH-independent bilayer thickness of PAH and strong polyanions below the pK_a-value of PAH.[20]

The layer-by-layer deposition can also be carried out with cationic SWNT-PEs and polyanions, e.g. with PSS, and to demonstrate this configuration, we have prepared multilayers of SWNT**3** and PSS. Working with cationic nanotubes is not as straightforward as with anionic ones because they easily precipitate during substrate incubation, probably due to the negatively charged glass surface. Therefore, special care was taken to replace the nanotube solution during the LbL procedure if necessary; these precautions ensure the formation of a homogeneous film. The SWNT**3**/PSS multilayer growth is linear although more irregular than that of SWNT**1**/PDADMA or SWNT**2**/PDADMA multilayers (Figure 1d), perhaps due to enhanced nanotube aggregation. In this case the methylimidazolium group in the ionic modifier **3** can exhibit cation$-\pi$ interactions with nanotubes, which increases the tendency of SWNT**3** to aggregate.[18] However, the results presented in Figure 1 show that SWNT/polyelectrolyte multilayers can be successfully prepared using either cationic or anionic SWNT-PEs and different polyelectrolytes of opposite charge. This makes possible the incorporation of SWNTs in arbitrary polyelectrolyte multilayers with a multitude of film structures and compositions.

SWNT/SWNT Multilayers. Most self-assembled SWNT films described in the literature have been prepared using oxidized nanotubes carrying negative charges and cationic polyelectrolytes, usually PDADMA. In a recent article Yan et al. used the LbL method for the self-assembly of PSS and cationic SWNTs prepared by noncovalent modification with methylene blue.[17] To our best knowledge, no work on the layer-by-layer self-assembly of all-SWNT multilayers has been reported. The anionic and cationic SWNT polyelectrolytes prepared by the noncovalent modification with compounds **1**−**4** offer a possibility to construct pure nanotube multilayers in a controlled fashion. To demonstrate this, we have fabricated SWNT/SWNT multilayers using oppositely charged nanotubes SWNT**1** or SWNT**2** and SWNT**3** or SWNT**4** by their alternate adsorption. Without any added electrolyte in the nanotube solutions the growth of SWNT**1**/SWNT**3** and SWNT**1**/SWNT**4** multilayers was very slow and irregular, although still discernible (see Supporting Information). However, the increase of the ionic strength in the anionic SWNT solutions to 0.10−0.15 M with NaBr accelerated the film growth, which became nearly linear and reproducible (Figure 2), and all-SWNT multilayers with several tens of nanotube layers have been fabricated using the layer-by-layer technique (vide infra). The S_{11} transitions were more suppressed and broadened in these SWNT/SWNT films than in the SWNT/polyelectrolyte multilayers, probably due to increased intertube interactions in all-SWNT films.

Pristine SWNTs are known to interact strongly with each other by van der Waals interactions. To exclude the possibility that the formation of SWNT/polyelectrolyte or SWNT/SWNT multilayers could be attributed to interactions between the unmodified regions of the SWNT sidewalls, control experiments were carried out. No multilayer growth was observed if the anionic SWNT**1** was used as the only component or with another polyanion, PSS (see Supporting Information). These results indicate that the formation of both SWNT/polyelectrolyte and SWNT/SWNT multilayers is primarily based on the electrostatic interactions, and the nanotube−nanotube interactions play only a minor or negligible role as the SWNT-PEs cannot be adsorbed on a surface carrying a similar charge.

General Discussion of the Layer-by-Layer Assembly with SWNTs. We have used the SWNT/PDADMA system as a model to characterize the LbL assembly process of carbon nanotube polyelectrolytes by various methods. With rigid-rod polyelectrolytes, such as water-soluble polythiophenes, the rigid polyelectrolyte layer is partly desorbed upon adsorption of the next layer.[21] This can be explained by the dissolution of the loosely bound, aggregated material in the form of soluble polyelectrolyte−polyelectrolyte complexes. To study the mechanism of the layer-by-layer assembly with SWNT-PEs, the layer growth was followed with surface plasmon resonance (SPR) and UV−vis−near-IR spectroscopy. The resonance angle of incidence, at which the reflectance minimum is observed, depends on changes in the optical thickness at the interface between the metal electrode and solution. To the first approximation, the thickness of the adsorbed layer is proportional to the change in the angle corresponding to the minimum. Figure 3 shows the changes in the resonance angle upon adsorption of anionic SWNT**1** on a MEA-treated gold surface. A rapid initial rise (ca. 70% of total net change in 5 min) is followed by a much slower change in the resonance angle, reminiscent of the general mode of behavior with both rigid-rod and flexible polyelectrolytes.[21] While the initial rise must result from a rapid adsorption of anionic nanotubes on the positively charged surface, the subsequent slower process may be caused by conformational changes in the adsorbed material or continued adsorption. Rinsing with the electrolyte solution rapidly restores the signal to the level initially obtained after ca. 40 min of adsorption, which strongly suggests that the further increase of the resonance angle is caused by slow adsorption of loosely bound nanotube material, possibly in the form of larger

(21) Lukkari, J.; Salomäki, M.; Ääritalo, T.; Loikas, K.; Laiho, T.; Kankare, J. *Langmuir* **2002**, *18*, 8496.

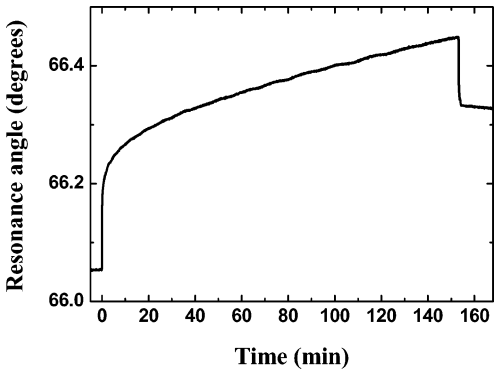

Figure 3. Change of the surface plasmon resonance angle during the adsorption of SWNT**1** on Au/MEA. The cell was initially filled with 0.1 M NaBr. At zero time a solution of SWNT**1** (in 0.1 M NaBr) was introduced into the cell. After 153 min the cell was rinsed with 0.1 M NaBr.

bundles or aggregates. Therefore, the amount corresponding to a full layer is adsorbed within 30−40 min.

Spectroscopic measurements at one-layer intervals support the conclusions above. Figure 4a shows the increase of absorbance at 1190 and 665 nm (in the range of the S_{11} and S_{22} transitions, respectively) after the deposition of each layer for a SWNT**1**/PDADMA multilayer. In the vis−near-IR spectral range PDADMA does not contribute to the increase of multilayer absorbance. The behavior at these two wavelengths was unexpectedly different. The absorbance increases steadily at 1190 nm, even after the addition of a PDADMA layer, but exhibits a more expected ladderlike behavior at 665 nm. In fact, the absorbance at 665 nm decreases upon addition of a PDADMA layer, producing a zigzag-type curve. The complete spectra (see Supporting Information) reveal that the change in behavior takes place in the spectral range 700−900 nm.

The decrease of absorbance below ca. 700 nm after the adsorption of each PDADMA layer cannot be explained by selective dissolution of metallic nanotubes, because the intensity of the M_{11} transitions does not change markedly when compared to S_{22} transitions. Instead, the decrease of absorbance implies that unselective desorption of nanotube material takes place during the incubation in the PDADMA solution. Therefore, the mechanism of the LbL assembly of SWNT-PEs also involves partial stripping of the nanotube layer upon adsorption of the next layer, possibly as small loosely attached nanotube bundles. The increase of absorbance above ca. 900 nm due to a PDADMA layer is more enigmatic. It cannot result from light scattering because this effect should be more pronounced at short wavelengths. We can also rule out the pH modulation of the S_{11} bands because the pH of both deposition solutions was kept at 6.2. The most probable explanation for the phenomenon is the desorption of the anionic naphthalene sulfonate modifiers from the nanotube surface into the PDADMA solution. The noncovalently adsorbed modifiers on the nanotube surface are in dynamic equilibrium with the solution species, and the stability of the aqueous nanotube solution is largely determined by this adsorption−desorption equilibrium. Thorough rinsing and, especially, a contact with a polycation solution favor the desorption of anionic modifiers. In fact, the reddish color of SWNT**2** (due to 5-aminonaphthalene-2-sulfonic acid **2**) was transferred to the PDADMA solution in the course of the SWNT**2**/PDADMA multilayer buildup. In our previous work, we have shown that the modified SWNTs are *n*-doped because of the charge transfer from adsorbates to the nanotubes.[18] The chemical *n*-doping shifts the Fermi level of undoped SWNTs upward by filling the states above the Fermi level, thus decreasing the intensity of the optical transition between the high-lying S_{11} van Hove singularities. Partial removal of the adsorbates partially undopes the nanotubes and increases the absorbance of the S_{11} band without significantly affecting the M_{11} or S_{22} transitions. On the other hand, in the case of SWNT/SWNT multilayers the zigzag behavior is not as evident (Figure 4b) as with the SWNT/PDADMA multilayer. Since the nanotubes are large objects, which can be suspended in water only with difficulty, the formation of soluble complexes between oppositely charged SWNT-PEs, leading to the partial desorption of the topmost layer, occurs only to a minor extent.

The stability of the nanotube solutions generally decreases with increased ionic strength, probably due to screening-induced aggregation. Therefore, the SWNT solutions used for the buildup of the SWNT/PDADMA multilayers in Figure 1 did not contain any added salt. However, the addition of salt to polyelectrolyte solutions has been shown to result in an improved layer growth. Different counterions have specific effects, and the influence of the anions has been shown to follow the Hofmeister (lyotropic) series.[22] In particular, the use of bromide anion in the LbL deposition of PSS/PDADMA multilayers produces thick and reproducible films. Therefore, the effect of the added electrolyte in the SWNT solution was studied with two parallel depositions, one with the salt (0.1 M NaBr) present in the SWNT**2** solution and another without any added salt. The PDADMA solutions were always 0.1 M with respect to NaBr, and all other deposition conditions were identical. The addition of salt in the nanotube solution has a profound effect on the multilayer formation (Figure 5). The increase of ionic strength results in a 2.5-fold increase in the total absorbance after 15 bilayers. As most of the absorbance is due to nanotube material (a small scattering background due to PDADMA may be included) this demonstrates that the amount of nanotubes in the film more than doubles due to the added salt. In addition, the film growth is linear in the presence of added electrolyte, whereas it exhibits a clear curvature without the added salt. Similar results were obtained with SWNT**1**/PDADMA multilayers (a 4.2-fold increase in the total absorbance, see Supporting Information). Layer growth turned linear at higher ionic strength also in this case. Therefore, the multilayer formation is profoundly affected by added electrolyte in the SWNT-PE/polyelectrolyte systems, too. However, with cationic SWNT**3** electrolyte addition could not be applied because of immediate precipitation of the nanotubes. This anion-induced precipitation of nanotubes was not studied further, but we tentatively suggest that interactions between the methylimidazolium group and the added anions may cause aggregation of the modified nanotubes in this case.[23] The addition of more than 0.2 M NaBr caused the formation of small SWNT aggregates with anionic nanotubes, too, showing that the water solutions of SWNT-PEs are labile at high ionic strength.

Ellipsometry was used to estimate the thickness of the multilayers. In previous works the dielectric functions of graphite or some other approximated values have been used with carbon nanotube films.[13,24] The surface-aligned nanotube films are anisotropic and their dielectric functions parallel to the tube axis closely resemble those of highly oriented pyrolytic graphite (HOPG), whereas the dielectric functions perpendicular to the axis cannot be reproduced using HOPG data.[25] Despite these complications we have used the isotropic dielectric functions of

(22) Salomäki, M.; Tervasmäki, P.; Areva, S.; Kankare, J. *Langmuir* **2004**, *20*, 3679.
(23) Itoh, H.; Naka, K.; Chujo, Y. *J. Am. Chem. Soc.* **2004**, *126*, 3026.
(24) Matsumoto, K.; Maeda, H.; Kawaguchi, Y.; Takahashi, K.; Aoyama, M.; Yamaguchi, T.; Postava, K. *Thin Solid Films* **2004**, *455*−*456*, 339.
(25) de Heer, W. A.; Bacsa, W. S.; Châtelain, A.; Gerfin, T.; Humphrey-Baker, R.; Forro, L.; Ugarte, D. *Science* **1995**, *268*, 845.

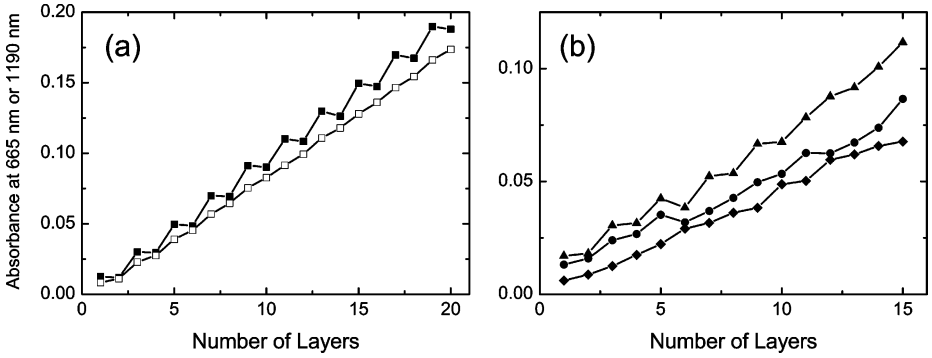

Figure 4. (a) Absorbance at 665 (solid squares) and 1190 nm (open squares) as a function of the number of layers for a SWNT**1**/PDADMA multilayer (even layers: PDADMA on top) and (b) absorbance at 665 nm as a function of the number of layers for SWNT**1**/SWNT**3** (circles), SWNT**1**/SWNT**4** (triangles), and SWNT**2**/SWNT**3** (diamonds) multilayers. The ionic strength of the anionic SWNT-PE solution was adjusted to 0.10−0.15 M with NaBr.

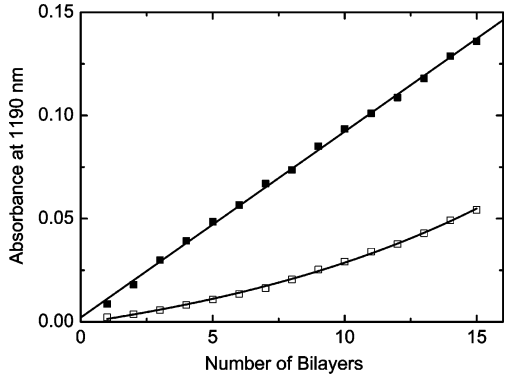

Figure 5. S_{11} peak absorbance (1190 nm) as a function of the number of bilayers for SWNT**2**/PDADMA multilayers. The ionic strength (adjusted with NaBr) in the SWNT**2** solutions was either zero (open symbols) or 0.1 M (solid symbols). Lines are shown as a guide to the eye.

graphite to approximate the optical properties of nanotube films. All the films have been modeled as mixtures of graphite and air using the Bruggemann effective medium approximation with air as the host and graphite as the inclusion material.[26] The volume fraction of inclusions and the layer thickness were used as fitting parameters. The model does not take into account the separate contributions of nanotubes and polymers, but it reproduces the experimental data sufficiently well. We emphasize that the thickness values calculated with this model should be considered as relative estimates because of the approximations involved. However, ellipsometry confirms the marked increase of the film thickness due to added electrolyte. The SWNT**2**/PDADMA multilayer deposited in the presence of NaBr gave a thickness of 36.0 nm after 14.5 bilayers, while the one prepared without salt was only 9.9 nm thick (for a comprehensive list of ellipsometric thickness and volume fraction determinations, see Table S1 in Supporting Information). Some other trends can also be seen in the ellipsometric thickness of various SWNT/polyelectrolyte films. The SWNT**2**/PDADMA multilayers were consistently thinner than the SWNT**1**/PDADMA films, in accordance with absorbance data and the higher surface charge density of SWNT**2**.[18] Multilayers of cationic SWNT**4** with PSS tend to become somewhat thicker, probably because of the tendency of PSS to self-aggregate.[27]

Theoretically, a perfectly aligned complete nanotube monolayer would give a mass density of ca. 0.12 μg/cm^2 (calculated for a monolayer consisting of parallel (12,0) or (7,7) nanotubes having the diameter of 0.95 nm).[28] Using the measured multilayer spectra and the average absorption coefficient of SWNT-PEs determined previously[18] (ca. 10 600 cm^2 g^{-1} at 925 nm), we can estimate the amount of nanotube material adsorbed per SWNT layer in the SWNT/polyelectrolyte and SWNT/SWNT multilayers. The nanotube loading per layer generally ranges between ca. 0.1−0.6 μg/cm^2 for SWNT/polyelectrolyte films prepared without added electrolyte in the nanotube solution, formally equivalent to the adsorption of 1−5 monolayers. Addition of salt (0.1 M NaBr) in the SWNT solution increases the amount of adsorbed nanotubes to 0.6−1.3 μg/cm^2 per layer. In all-SWNT multilayers the loading is approximately 0.12 μg/cm^2 per nanotube layer without added electrolyte and the addition of salt (0.1−0.2 M NaBr) in the anionic nanotube solution increases the loading to 0.3 ± 0.1 μg/cm^2. The SWNT/SWNT multilayers are also generally thinner than the SWNT/polyelectrolyte films, which can be attributed to the relatively high rigidity and linear geometry of the nanotubes, compared with conventional polyelectrolytes. The nanotubes, therefore, tend to lie flat on the surface and do not form loops or tails protruding into the solution. The average film thickness increase per layer is around 1 nm for the all-SWNT films, which is close to the average diameter of the HiPco nanotubes used, suggesting that approximately a monolayer of nanotubes is adsorbed at each cycle, in accordance with the observed mass loading. With SWNT/polyelectrolyte multilayers, especially with added salt, the thickness increments are clearly larger, approximately 3 ± 1 nm *per* bilayer, similar to the SWNT/polymer films reported previously (1.5−2 nm *per* bilayer).[13,15] In general, however, thickness is not a very sensitive measure of the amount of material on a rough surface. While the addition of salt in the nanotube solution greatly influences the LbL assembly of SWNT/polyelectrolyte films the increase of the ionic strength of the anionic SWNT solution from zero to 0.1 M increases the SWNT/SWNT film thickness only very little. Further increase of the ionic strength has a negligible effect. This behavior is similar to that observed with water-soluble ionic polythiophenes and seems to be a general phenomenon with rigid rodlike polyelectrolytes.[21] It is well-known that polyelectrolyte multilayers are not stratified structures, and the individual layers strongly interpenetrate the adjacent layers. We have previously shown that rigid-rod polythiophenes can penetrate 6−9 layers, depending on the ionic strength of the solution and the type of

(26) Tompkins, H. G.; McGahan, W. A. *Spectroscopic Ellipsometry and Reflectometry. A User's Guide*; John Wiley & Sons: New York, 1999.

(27) (a) Tanahatoe, J. T.; Kuil, M. E. *J. Phys. Chem. B* **1997**, *101*, 5905. (b) Tanahatoe, J. T.; Kuil, M. E. *J. Phys. Chem. B* **1997**, *101*, 9233. (c) Tanahatoe, J. T.; Kuil, M. E. *J. Phys. Chem. B* **1997**, *101*, 10839.

(28) Dresselhaus, M. S.; Dresselhaus, G.; Saito, R. *Carbon* **1995**, *33*, 883.

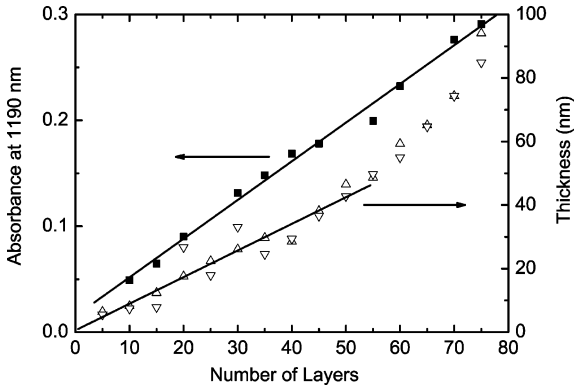

Figure 6. SWNT**1**/SWNT**4** multilayer growth (on glass) up to 75 layers. Film growth was followed by vis−near-IR spectroscopy (solid squares), variable-angle ellipsometry (triangles pointing up) and spectroscopic ellipsometry (triangles pointing down). Salt (0.1 M NaBr) was added to the SWNT**1** solution. Linear fits to the spectroscopic data and initial thickness growth are shown.

polyelectrolytes.[29] The ionic strength in the solution of the incoming polyelectrolyte solution modifies the existing film, and increasing the small electrolyte concentration makes the film more permeable to the adsorbing polyelectrolyte. Similarly, the penetration depth of conventional polyelectrolytes has been shown to be a function of the ionic strength.[30] The small electrolytes in the adsorption solution break the ion−ion pairs between the polyelectrolytes in the existing multilayer, swell the film, and allow better penetration and incorporation of the incoming polyelectrolyte, thus increasing the amount of adsorbed material and multilayer thickness.[31] The multilayers consisting solely of rigid-rod components swell to a much smaller extent, which explains the insensitivity of SWNT/SWNT (and all-thiophene) multilayers to the ionic strength of the adsorption solutions. However, it is possible to fabricate SWNT/SWNT films having several tens of layers, and the growth of a 75-layer film composed of SWNT**1** and SWNT**4** is shown in Figure 6. The increase of the nanotube material is linear, as judged by the absorbance data. The film thickness was studied by ellipsometry at 5-layer intervals, and variable-angle and spectroscopic ellipsometry both gave consistent results. The thickness increases first linearly (at a rate of ca. 0.75 nm/SWNT layer), too, but curves upward (approximately to 2 nm/SWNT layer) when the number of layers exceeds ca. 40−50, probably reflecting the loss of order and increase of surface roughness in thick multilayers. This conclusion is supported by the rapid increase of macroscopic roughness in all-SWNT films as determined by imaging ellipsometry (vide infra). In all multilayers the volume fraction of nanotubes and polyelectrolyte is ca. 0.5 in the beginning but decreases with film thickness and stabilizes at a value of 0.35 ± 0.10 after ca. 10 layers, suggesting a slight decrease of film density after the initial layers (zone I).

The surface morphology of the SWNT/polyelectrolyte and SWNT/SWNT films was studied with AFM and SEM. The multilayers were prepared on silicon substrates, which were cleaned and silanized similarly to the glass substrates in order to ensure comparable deposition conditions. Figure 7 shows the AFM images of SWNT**2**/PDADMA, PSS/SWNT**3**, and SWNT**2**/SWNT**3** multilayers. Random networks of nanotube bundles oriented parallel to the surface are visible in all films, and the surface density of nanotubes increases with the number of layers.

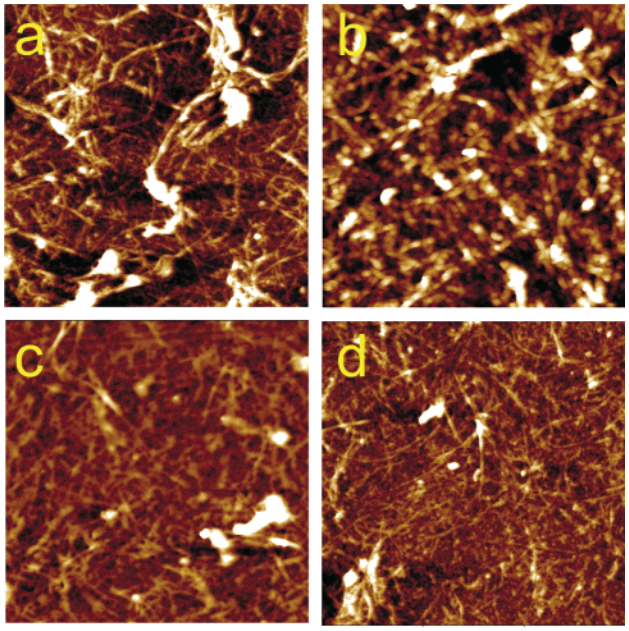

Figure 7. AFM images of (a) (SWNT**2**/PDADMA)$_4$/SWNT**2**, (b) (SWNT**2**/PDADMA)$_9$/SWNT**2**, (c) (PSS/SWNT**3**)$_{10}$, and (d) (SWNT**2**/SWNT**3**)$_5$ multilayers. The imaged area is 3 × 3 μm^2, and the *z* scale is 50 nm. The average bundle size (analyzed over 20−60 bundles; average and standard deviation) is (a) 46 ± 9, (b) 84 ± 11, (c) 61 ± 10, and (d) 40 ± 10 nm.

This is in accordance with previous results, which suggest that SWNT-PE solutions contain thin nanotube bundles.[18] Images obtained on films capped with either SWNT or polyelectrolyte (not shown) show that the nature of the topmost layer does not have any appreciable effect on the surface morphology. The average diameter of the bundles was estimated from the AFM images (20−60 analyzed bundles per image); the results from the SEM images (not shown) are consistent. The bundle size increases with film thickness, but there is only a small difference between the average bundle size of the two SWNT/polyelectrolyte multilayers studied. The ropelike appearance of the multilayer surface supports the idea that flexible PDADMA or PSS molecules tend to coat the oppositely charged nanotube surfaces, resulting in a somewhat hazy surface seen in the images, instead of forming separate intact layers alternately with the nanotubes. Similar "greasy" nanotubes were reported in SWNT/PEI and SWNT/PDADMA multilayers.[11,15] The nanotubes and, especially, nanotube bundles, represent semimacroscopic platforms (with respect to the individual polymer molecules) for self-assembly and wrapping of flexible polymers around nanotubes seems to be a general phenomenon.[32] In fact, attached individual SWNTs have been used as templates for the polyelectrolyte multilayer self-assembly.[16] In the SWNT/SWNT multilayer the bundles are thinner than in SWNT/polyelectrolyte films with a similar number of nanotube layers and have also sharper boundaries. In addition, the thinnest bundles have a diameter of ca. 20 nm, whereas the smallest diameters observed in other films are approximately 30−60 nm. Flexible PDADMA and PSS probably act as efficient glue binding nanotubes together. In well-interpenetrated and porous multilayers this provides a tentative mechanism for the average bundle growth with the number of layers.

The large-scale homogeneity of the SWNT/polyelectrolyte multilayers can be studied by imaging ellipsometry over macroscopic areas. The multilayers were imaged over an area of 2 × 3 mm^2 in order to estimate the film thickness and surface

(29) Lukkari, J.; Salomäki, M.; Viinikanoja, A.; Ääritalo, T.; Paukkunen, J.; Kocharova, N.; Kankare, J. *J. Am. Chem. Soc.* **2001**, *123*, 6083.
(30) Schlenoff, J. B.; Dubas, S. T. *Macromolecules* **2001**, *34*, 592.
(31) Salomäki, M.; Vinokurov, I. A.; Kankare, J. *Langmuir* **2005**, *21*, 11232.
(32) Baskaran, D.; Mays, J. W.; Bratcher, M. S. *Chem. Mater.* **2005**, *17*, 3389.

Table 1. Ellipsometric Mapping of the SWNT Multilayers

sample[a,b]	ionic strength[c] (M)	layers	mapped thickness[d] (nm)
SWNT**1**/PDADMA[a]	0.1	15	24.5 ± 6.8
SWNT**2**/PDADMA[a]	0.1	15	20.4 ± 0.6
PSS/SWNT**4**[a]	0	15	33.4 ± 1.9
SWNT**2**/PDADMA[b]	0.1	29	23.3 ± 2.2
SWNT**1**/SWNT**3**[a]	0	15	12.5 ± 2.3
SWNT**1**/SWNT**3**[a]	0.1	15	15.2 ± 2.5
SWNT**2**/SWNT**3**[a]	0.1	15	19.9 ±15.2
SWNT**1**/SWNT**4**[b]	0.1	60	58.1 ± 5.7
SWNT**1**/SWNT**4**[b]	0.1	75	88.5 ± 19.5

[a] On gold. [b] On glass. [c] Concentration of NaBr used with SWNT**1** or SWNT**2**. With PDADMA and PSS ionic strength was always 0.1 M; with SWNT**3** and SWNT**4** it was zero. [d] Mean thickness and root-mean-square roughness along a 2 mm profile. Volume fraction was fixed at the value obtained by spectroscopic ellipsometry.

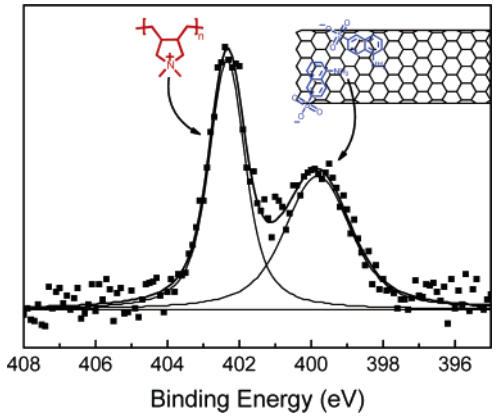

Figure 8. N 1s core level spectrum of a SWNT**2**/PDADMA multilayer with 9 layers (squares). Deconvoluted peaks (thin lines, Voigt line shape) and their sum curve (thick line) are shown.

roughness on a macroscopic scale (Table 1). Examples of the thickness maps of several SWNT/polyelectrolyte and SWNT/SWNT multilayers are shown in the Supporting Information. On this macroscopic scale, the surface roughness of the multilayers depends on the components used, and, especially, SWNT**2**/PDADMA and PSS/SWNT**4** multilayers exhibit macroscopically smooth surfaces. In general, the macroscopic roughness of both types of multilayers, SWNT/polyelectrolyte and SWNT/SWNT, is small with the exception of the SWNT**2**/SWNT**3** film. At the moment, we do not have an explanation for the high roughness of this multilayer. The surface roughness increases markedly in thick multilayers as seen from the results for the films with 60 and 75 layers.

Finally, to clarify the primary interactions responsible for the layer-by-layer assembly with SWNT-PEs, we have studied the stoichiometry and composition of the multilayers by XPS. Carbon, oxygen, nitrogen, and sulfur (and silicon from the substrate) could be seen in the survey spectra of a (SWNT**2**/PDADMA)$_4$/SWNT**2** multilayer (see Supporting Information). The charge stoichiometry in the multilayers can be assessed using the N 1s core level spectrum, which shows two components at 399.8 and 402.3 eV corresponding to the uncharged nitrogen in **2** and the charged nitrogen in PDADMA, respectively (Figure 8). In the XPS spectra of SWNT**2** or PDADMA only one N 1s peak is seen at 400.0 or 402.5 eV, respectively (for PDADMA, see Supporting Information). The relative amount of positively charged nitrogen (in PDADMA) is always 2−8 percentage units higher than that of the uncharged nitrogen in SWNT**2** (equivalent to the amount of anionic sulfonate groups), instead of the theoretical value of 50% expected for total intrinsic charge compensation in the multilayer. However, the close equivalence of the amounts of the components indicates that electrostatic ion pairs constitute the major interaction within the multilayers. Several factors may contribute to the observed surplus of charged nitrogens in these films. The results above show that incoming PDADMA layers and extensive rinsing remove part of the noncovalently adsorbed ionic modifiers on the SWNT surface. Therefore, part of the ionic charges of PDADMA will be compensated for by small anions in solution.[21,33] It is, however, noteworthy that no bromine was detected by XPS in the SWNT**2**/PDADMA multilayers, although it compensates for approximately one-third of the quaternary ammonium charges throughout the PSS/PDADMA multilayers.[33] On the other hand, several polymers have been shown to tightly wrap around carbon nanotubes,[32,34] and charged nanotubes act as efficient templates for polyelectrolytes.[16] Therefore, we tentatively assume that the wrapping of flexible PDADMA molecules around the relatively rigid SWNTs favors polyelectrolyte−polyelectrolyte charge compensation and expulsion of small counteranions that initially compensate the charges in PDADMA. Another reason for the lack of bromide in the SWNT-containing multilayers can be their higher porosity as compared to the conventional polyelectrolyte multilayers. Finally, it should be pointed out that PDADMA−nanotube interactions have recently been suggested to stem from unsaturated impurities in PDADMA, resulting from the polymerization process.[14] These impurities were detected by the $\pi-\pi$ shake-up in the C 1s XPS spectrum of PDADMA, which disappeared upon interaction with nanotubes. However, our PDADMA shows no $\pi-\pi$ shake-up features (see Supporting Information), and although this suggested $\pi-\pi$ interaction could also partly explain the excess of charged nitrogen in the multilayers, we have found no evidence for such interactions in our SWNT/PDADMA films.

Conclusions

Noncovalently modified single-wall carbon nanotubes carrying anionic or cationic groups, single-wall carbon nanotube polyelectrolytes (SWNT-PEs), can be used for the preparation of thin films by the layer-by-layer self-assembly technique in an aqueous medium. This is a very general and powerful technique for the fabrication of thin carbon nanotube films of arbitrary composition and architecture. Only polycations can be assembled with oxidized (and cut) nanotubes having negative carboxylate groups, but SWNT-PEs allow the use of both cationic and anionic polyelectrolytes for the generation of SWNT/polyelectrolyte multilayers. In addition, in these multilayers nanotubes retain their electronic structure intact. Most importantly, also SWNT/SWNT films can be self-assembled layer-by-layer without any non-nanotube components.

The charge compensation in these SWNT multilayers is intrinsic, which shows that electrostatic interactions are mainly responsible for the multilayer buildup. Part of the topmost nanotube layer is desorbed upon adsorption of the next polyelectrolyte layer, but the film growth is linear after the initial layers. In SWNT/polyelectrolyte multilayers, the film growth can be markedly accelerated by increasing the ionic strength of the SWNT solution, but for all-SWNT multilayers the increase of ionic strength has only a small effect, in accordance with other rigid-rod polyelectrolytes. The amount of nanotube material deposited per layer varies between 1 and 5 theoretical SWNT

(33) Salomäki, M.; Laiho, T.; Kankare, J. *Macromolecules* **2004**, *37*, 9585.
(34) (a) O'Connell, M. J.; Boul, P. J.; Ericson, L. M.; Huffman, C. B.; Wang, Y.; Haroz, E. H.; Kuper, C.; Tour, J. M.; Ausman, K. D.; Smalley, R. E. *Chem. Phys. Lett.* **2001**, *342*, 265. (b) Star, A.; Liu, Y.; Grant, K.; Ridvan, L.; Stoddart, J. F.; Steuerman, D. W.; Diehl, M. R.; Boukai, A.; Heath, J. R. *Macromolecules* **2003**, *36*, 553.

monolayers in SWNT/polyelectrolyte films without added electrolyte in the SWNT solution, whereas it is only 1−2 monolayers for all-SWNT films, in accordance with the ca. 1 nm layer thickness observed by ellipsometry. The surface of both SWNT/polyelectrolyte and SWNT/SWNT multilayers displays a random network of small nanotube bundles lying flat on the surface. The average bundle size mainly depends on the film thickness, and flexible polyelectrolytes seem to cover the nanotubes and bind them together, the smallest bundles being observed in all-SWNT multilayers. The homogeneity of the multilayers on a macroscopic scale was studied with imaging ellipsometry. On this scale, the surface roughness depends on the film thickness and its components, ranging from smooth to very rough.

The electrostatic layer-by-layer self-assembly of SWNT-PEs is a feasible method to fabricate carbon nanotube films with thickness from a few nanometers to tens or hundreds of nanometers, containing several tens or hundreds of nanotube layers. The incorporation of other components can be done as easily as with other polyelectrolyte multilayers. The process is carried out entirely in aqueous medium, which is important for biocompatibility and offers, therefore, a possibility for an environmental-friendly, solvent-free method for the fabrication of carbon nanotube films and composites.

Acknowledgment. Financial aid from the Academy of Finland (Grant 50537) and the Graduate School of Materials Research (Turku, Finland) is gratefully acknowledged. We thank Prof. Jouko Kankare and Mr. Mikko Salomäki for valuable discussions.

Supporting Information Available: Additional spectroscopic results for SWNT/polyelectrolyte and SWNT/SWNT multilayer growth on glass, table of ellipsometric thickness and volume fraction determinations, ellipsometric thickness maps of SWNT/polyelectrolyte and SWNT/SWNT multilayers on glass and gold, XPS survey spectra and atomic composition of SWNT**2**/PDADMA multilayers on silicon, and the C 1s core level spectrum of a PDADMA monolayer on gold. This material is available free of charge via the Internet at http://pubs.acs.org.

LA051736I